

Production of $X(3872)$ Accompanied by a Pion in B Meson Decay

Eric Braaten,* Li-Ping He,[†] and Kevin Ingles[‡]

Department of Physics, The Ohio State University, Columbus, OH 43210, USA

(Dated: November 5, 2021)

Abstract

If the $X(3872)$ is a weakly bound charm-meson molecule, it can be produced by the creation of $D^{*0}\bar{D}^0$ or $D^0\bar{D}^{*0}$ at short distances followed by the formation of the bound state from the charm-meson pairs. It can also be produced by the creation of $D^*\bar{D}^*$ at short distances followed by the rescattering of the charm mesons into $X\pi$. We use results of a previous isospin analysis of B meson decays into $KD^{(*)}\bar{D}^{(*)}$ to estimate the short-distance amplitudes for creating $D^*\bar{D}^*$. We use an effective field theory for charm mesons and pions called XEFT to calculate the amplitudes for rescattering of $D^*\bar{D}^*$ into $X\pi$ with small relative momentum. The $X\pi$ invariant mass distribution is predicted to have a narrow peak near the $D^*\bar{D}^*$ threshold from a charm-meson triangle singularity. We estimate the branching fractions into the peak from the triangle singularity for the decays $B^0 \rightarrow K^+ X\pi^-$ and $B^+ \rightarrow K^0 X\pi^+$.

PACS numbers: 14.80.Va, 67.85.Bc, 31.15.bt

Keywords: Exotic hadrons, charm mesons, effective field theory.

* braaten.1@osu.edu

[†] he.1011@buckeyemail.osu.edu

[‡] ingles.27@buckeyemail.osu.edu

I. INTRODUCTION

The discovery of a large number of exotic hadrons containing a heavy quark and its antiquark presents a major challenge to our understanding of QCD [1–10]. The $X(3872)$ meson was the first of these exotic hadrons to be discovered. It is the one for which the most data is available, but there is still no consensus on its nature. The X was discovered in 2003 by the Belle collaboration in exclusive decays of B^\pm mesons into $K^\pm X$ through its decay into $J/\psi \pi^+ \pi^-$ [11]. The observation of its decay into $J/\psi \pi^+ \pi^- \pi^0$ revealed a dramatic violation of isospin symmetry [12]. The X has also been observed in the decay modes $D^0 \bar{D}^0 \pi^0$, $D^0 \bar{D}^0 \gamma$, $J/\psi \gamma$, $\psi(2S) \gamma$, and $\chi_{c1} \pi^0$. The J^{PC} quantum numbers of X were eventually determined to be 1^{++} [13]. Its mass is extremely close to the $D^{*0} \bar{D}^0$ threshold, with the difference being only 0.01 ± 0.18 MeV [14]. This suggests that X is a weakly bound S-wave charm-meson molecule with the flavor structure

$$|X(3872)\rangle = \frac{1}{\sqrt{2}} \left(|D^{*0} \bar{D}^0\rangle + |D^0 \bar{D}^{*0}\rangle \right). \quad (1)$$

There are alternative models for the X [1–10], but the observation of X in 7 different decay modes has not been effective in discriminating between these models. However there may be aspects of the production of X that are more effective at discriminating between models than the decays of X .

A convenient theoretical framework for describing X as a weakly bound charm-meson molecule is an effective field theory for charm mesons and pions called XEFT [15]. It describes the sector of QCD consisting of $D^* \bar{D}$, $D \bar{D}^*$, and $D \bar{D} \pi$ with small relative momenta as well as the weakly bound state X . In Ref. [16], it was pointed out that XEFT could also be applied to the sector of QCD consisting of $D^* \bar{D}^*$, $D \bar{D}^* \pi$, $D^* \bar{D} \pi$, $D \bar{D} \pi \pi$, and $X \pi$. XEFT can be applied to the production of X from short-distance processes that create a pair of charm mesons. If a high energy reaction creates $D^{*0} \bar{D}^0$ and $D^0 \bar{D}^{*0}$ at short distances, XEFT can describe their binding into X . If a high energy reaction creates $D^* \bar{D}^*$ at short distances, XEFT can describe their rescattering into $X \pi$.

In Ref. [17], we pointed out that the prompt production of X accompanied by a pion could be important at a hadron collider. We calculated the cross sections for inclusive production of $X \pi^\pm$ and $X \pi^0$ with small relative momentum. The calculations took advantage of cancellations of interference effects from the sum over the many additional particles in the inclusive cross sections. The $X \pi$ invariant mass distribution has a narrow peak near the $D^* \bar{D}^*$ threshold. In retrospect, these narrow peaks come from triangle singularities [18–21]. The corresponding Feynman diagrams have three charm meson lines that form a triangle, and this results in a kinematic singularity from the region where all three charm mesons are on-shell.

Guo recently pointed out that if a short-distance process can create an S-wave $D^* \bar{D}^*$ pair, it will produce a narrow peak in the $X \gamma$ invariant mass distribution near the $D^* \bar{D}^*$ threshold from a charm-meson triangle singularity [22]. Dubinskiy and Voloshin pointed out previously that $e^+ e^-$ annihilation will produce a narrow peak in the $X \gamma$ invariant mass distribution from rescattering of a P-wave $D^{*0} \bar{D}^{*0}$ pair [23]. The peak comes from a charm-meson triangle singularity. In Ref. [24], we predicted the normalized cross section near the peak, and we showed that the peak may be large enough to be observed by the BESIII detector.

Another short-distance process that can create a $D^* \bar{D}^*$ pair is B meson decay. In this paper, we study exclusive decays of B mesons into $K X \pi$ through the decay into $K D^* \bar{D}^*$ at

short distances followed by the rescattering of $D^*\bar{D}^*$ into $X\pi$. In Section II, we summarize previous work on the effective field theory XEFT. In Section III, we describe a precise isospin analysis of the decays $B \rightarrow KD^{(*)}\bar{D}^{(*)}$ by Poireau and Zito [25]. In Section IV, we verify that measurements for $B \rightarrow KX$ are compatible with the isospin amplitudes of Poireau and Zito for decays into $KD^{*0}\bar{D}^0$ and $KD^0\bar{D}^{*0}$. In Section V, we construct interaction terms for $B \rightarrow KD^{(*)}\bar{D}^{(*)}$ in which the $c\bar{c}$ pair in the charm mesons are in a spin-triplet state when the relative momentum of the charm mesons is 0. In Section VI, we use XEFT to calculate the rates for producing $D^*\bar{D}^*$ near the threshold. In Section VII, we use XEFT to calculate the rates for the rescattering of $D^*\bar{D}^*$ into $X\pi$. We conclude in Section VIII with a discussion of our results.

II. XEFT

The difference between the mass of the $X(3872)$ and the energy of the $D^{*0}\bar{D}^0$ scattering threshold is [14]

$$E_X \equiv M_X - (M_{*0} + M_0) = (+0.01 \pm 0.18) \text{ MeV}. \quad (2)$$

We denote the masses of the spin-0 charm mesons D^0 and D^+ by M_0 and M_1 (or collectively by M_D), the masses of the spin-1 charm mesons D^{*0} and D^{*+} by M_{*0} and M_{*1} (or collectively by M_{D^*}), and the masses of the pions π^0 and π^+ by m_0 and m_1 (or collectively by m_π). The reduced mass of D^{*0} and \bar{D}^0 is $\mu = M_{*0}M_0/(M_{*0} + M_0)$. The central value in Eq. (2) corresponds to on-shell charm mesons, which would require the X to be a virtual state rather than a bound state. The value lower by 1σ corresponds to a bound state with binding energy $|E_X| = 0.17$ MeV and binding momentum $\gamma_X \equiv \sqrt{2\mu|E_X|} = 18$ MeV.

If short-range interactions produce an S-wave bound state very close to the scattering threshold for its constituents, the few-body physics has universal aspects determined by the binding momentum γ_X [26]. The universal wavefunction for the constituents of the bound state to have relative momentum k small compared to the inverse range is

$$\psi_X(k) = \frac{\sqrt{8\pi\gamma_X}}{k^2 + \gamma_X^2}. \quad (3)$$

The universal scattering amplitude for the elastic scattering of the constituents with relative momentum k small compared to the inverse range is

$$f_X(k) = \frac{1}{-\gamma_X - ik}. \quad (4)$$

The universal results in Eqs. (3) and (4) can be derived from a *zero-range effective field theory* [27]. In the case of the X , it is a nonrelativistic effective field theory (EFT) for the neutral charm mesons D^{*0} , \bar{D}^{*0} , D^0 , and \bar{D}^0 . This EFT describes explicitly the $D^{*0}\bar{D}^0$ and $D^0\bar{D}^{*0}$ components of the X . Since the EFT does not describe charged charm mesons explicitly, its range of validity extends in energy at most up to the $D^{*+}D^-$ scattering threshold, which is higher than the $D^{*0}\bar{D}^0$ scattering threshold by 8.2 MeV. This EFT does not describe explicitly the $D^0\bar{D}^0\pi^0$ component of the X , which can arise from the decays $D^{*0} \rightarrow D^0\pi^0$ or $\bar{D}^{*0} \rightarrow \bar{D}^0\pi^0$.

Fleming, Kusunoki, Mehen and van Kolck developed a nonrelativistic effective field theory called *XEFT* with a much greater range of validity than the zero-range EFT, because it

describes pion interactions explicitly [15]. It is an EFT for neutral and charged S-wave charm mesons D^* , \bar{D}^* , D , and \bar{D} and for neutral and charged pions π . The number of charm mesons D and D^* and the number of anti-charm mesons \bar{D} and \bar{D}^* are conserved in XEFT. The contact interactions among the charm-meson pairs $D^*\bar{D}$ and $D\bar{D}^*$ in the $J^{PC} = 1^{++}$ channel with total electric charge 0 must be treated nonperturbatively in XEFT, but the coupling constant for pion interactions is small enough that the transitions $D^* \leftrightarrow D\pi$ can be treated perturbatively [15]. XEFT describes explicitly the $D^*\bar{D}$, $D\bar{D}^*$, and $\bar{D}D\pi$ components of the X . If a high energy process creates $D^{*0}\bar{D}^0$ and $D^0\bar{D}^{*0}$ at short distances, XEFT can describe the subsequent formation of X by the binding of the charm mesons. The region of validity of the original formulation of XEFT extends up to about the minimum energy required to produce a ρ meson. For a charm meson pair, this corresponds to a relative momentum greater than 1000 MeV. For a charm meson pair plus a pion, the region of validity of XEFT is also limited by the nonrelativistic approximation for the pion: the relative momentum of the pion must be less than about $m_\pi \approx 140$ MeV. We refer to a pion with relative momentum of order m_π or smaller as a *soft pion*.

Although pion interactions can be treated perturbatively in XEFT, they can also be treated nonperturbatively. The $D\bar{D}\pi$ components of the X have been taken into account with nonperturbative pion interactions by solving Faddeev integral equations [28]. The intensively numerical character of this approach makes it difficult to extract simple physical predictions.

A Galilean-invariant formulation of XEFT that exploits the approximate conservation of mass in the transitions $D^* \leftrightarrow D\pi$ was developed in Ref. [29]. In Galilean-invariant XEFT, the spin-0 charm mesons D^0 and D^+ have the same kinetic mass M_0 , the spin-1 charm mesons D^{*0} and D^+ have the same kinetic mass $M_0 + m_0$, and the pions π^0 and π^+ have the same kinetic mass m_0 . The difference between the physical mass and the kinetic mass of a particle is taken into account through its rest energy. The pion number defined by the sum of the numbers of D^* , \bar{D}^* , and π mesons is conserved in Galilean-invariant XEFT. The region of validity of Galilean-invariant XEFT extends up to about the minimum energy required to produce an additional pion, which is above the $D^*\bar{D}$ threshold by about 140 MeV. Galilean invariance also simplifies the ultraviolet divergences of XEFT.

An alternative Galilean-invariant EFT for S-wave charm mesons and pions that may be more predictive has been introduced by Schmidt, Jansen, and Hammer [30]. The only fields in this EFT are those for the spin-0 charm mesons D and the pions π . The spin-1 charm mesons D^* arise dynamically as P-wave $D\pi$ resonances.

In Ref. [16], Braaten, Hammer, and Mehen pointed out that XEFT could also be applied to sectors with pion number larger than 1. In particular, it can be applied to the sector with pion number 2, which consists of $D^*\bar{D}^*$, $D\bar{D}^*\pi$, $D^*\bar{D}\pi$, $D\bar{D}\pi\pi$, and $X\pi$. The cross sections for $D^*\bar{D}^* \rightarrow D^*\bar{D}^*$ and $D^*\bar{D}^* \rightarrow X\pi$ at small kinetic energies were calculated in Ref. [16]. If a high energy process can create $D^*\bar{D}^*$ at short distances, XEFT can describe their subsequent rescattering into X plus a soft pion. The inclusive prompt production of X plus a soft pion in high-energy hadron collisions was discussed in Ref. [17]. In this paper, we consider the production of X plus a soft pion in the exclusive decay of a B meson into $KX\pi$.

III. DECAYS INTO K PLUS A CHARM-MESON PAIR

A B meson can decay into a kaon and a pair of charm mesons. The symmetries of QCD provide constraints on the matrix elements for the decays $B \rightarrow KD^{(*)}\bar{D}^{(*)}$. The only exact symmetry is Lorentz invariance, which requires a matrix element to be a Lorentz-scalar function of the 4-momenta k , p , and \bar{p} of K , $D^{(*)}$, and $\bar{D}^{(*)}$ and the polarization 4-vectors ε and $\bar{\varepsilon}$ of D^* and \bar{D}^* . If the square of the matrix element is summed over the spins of any spin-1 charm mesons D^* or \bar{D}^* , it reduces to a function of the invariant masses $(p + \bar{p})^2$ of $D^{(*)}\bar{D}^{(*)}$ and $(k + p)^2$ of $KD^{(*)}$. The graphical representation of the dependence on these two variables is called a *Dalitz plot*.

The approximate isospin symmetry of QCD provides strong constraints on the matrix elements for the decays $B \rightarrow KD^{(*)}\bar{D}^{(*)}$. Each of the particles in such a reaction is a member of an isospin doublet. At the quark level, the decays for B^+ and B^0 are $\bar{b}q_1 \rightarrow (\bar{s}q_2)(c\bar{q}_3)(\bar{c}q_4)$, where each q_i is u or d . The isospin doublets for the light quarks and antiquarks are

$$\begin{pmatrix} u \\ d \end{pmatrix}, \quad \begin{pmatrix} -\bar{d} \\ \bar{u} \end{pmatrix}. \quad (5)$$

The isospin doublets for the B meson, the kaon, and the spin-0 charm mesons D and \bar{D} are

$$\begin{pmatrix} B^+ \\ B^0 \end{pmatrix}, \quad \begin{pmatrix} K^+ \\ K^0 \end{pmatrix}, \quad \begin{pmatrix} -D^+ \\ D^0 \end{pmatrix}, \quad \begin{pmatrix} \bar{D}^0 \\ D^- \end{pmatrix}. \quad (6)$$

The isospin doublets for the spin-1 charm mesons D^* and \bar{D}^* are analogous to those for D and \bar{D} . The $SU(2)$ isospin symmetry reduces the matrix elements to two complex amplitudes for each of the 4 sets of channels KDD , $KD^*\bar{D}$, $KD\bar{D}^*$, and $KD^*\bar{D}^*$. One choice for the isospin amplitudes A_0 and A_1 corresponds to $D^{(*)}K$ in an isospin-singlet and isospin-triplet state, respectively.

The expressions for the decay rates for $B \rightarrow KD^{(*)}\bar{D}^{(*)}$ in terms of dimensionless Lorentz-invariant matrix elements \mathcal{A} are

$$\Gamma[B \rightarrow KD^{(*)}\bar{D}^{(*)}] = \frac{1}{2M_B} \int d\Phi_{KD^{(*)}\bar{D}^{(*)}} \left| \mathcal{A}[B \rightarrow KD^{(*)}\bar{D}^{(*)}] \right|^2, \quad (7)$$

where M_B is the mass of the B meson and $d\Phi_{KD^{(*)}\bar{D}^{(*)}}$ is the differential phase space for the three mesons in the final state. Factors of 3 from summing over spins of D^* or \bar{D}^* are absorbed into the amplitudes \mathcal{A} . Using isospin symmetry, the amplitudes for the decays of B into $KD^{*0}\bar{D}^0$ and $KD^0\bar{D}^{*0}$ can be expressed in terms of 4 complex isospin amplitudes [31]:

$$\mathcal{A}[B^0 \rightarrow K^0 D^{*0} \bar{D}^0] = -\sqrt{\frac{2}{3}} A_1^{L*}, \quad (8a)$$

$$\mathcal{A}[B^0 \rightarrow K^0 D^0 \bar{D}^{*0}] = -\sqrt{\frac{2}{3}} A_1^{*L}, \quad (8b)$$

$$\mathcal{A}[B^+ \rightarrow K^+ D^{*0} \bar{D}^0] = \sqrt{\frac{1}{6}} A_1^{L*} + \sqrt{\frac{1}{2}} A_0^{L*}, \quad (8c)$$

$$\mathcal{A}[B^+ \rightarrow K^+ D^0 \bar{D}^{*0}] = \sqrt{\frac{1}{6}} A_1^{*L} + \sqrt{\frac{1}{2}} A_0^{*L}. \quad (8d)$$

These four amplitudes will be applied to the decays $B \rightarrow KX(3872)$ in Section IV. The amplitudes for the decays $B \rightarrow KD^*\bar{D}^*$ can be expressed in terms of 2 complex isospin

	$ A_0 \times 10^5$	$ A_1 \times 10^5$	δ
L^*	1.33 ± 0.04	0.42 ± 0.04	0.925 ± 0.157
$*L$	0.92 ± 0.03	0.41 ± 0.04	1.798 ± 0.122
$**$	2.28 ± 0.08	0.72 ± 0.05	1.745 ± 0.122

TABLE I. Amplitudes for $B \rightarrow K\bar{D}^{(*)}D^{(*)}$ decays from Ref. [25]. The rows labeled L^* , $*L$, and $**$ correspond to the $D^*\bar{D}$, $D\bar{D}^*$, and $D^*\bar{D}^*$ channels, respectively. The complex phase $e^{i\delta}$ of A_1/A_0 defines the angle δ .

amplitudes [31]:

$$\mathcal{A}[B^0 \rightarrow K^0 D^{*0} \bar{D}^{*0}] = -\sqrt{\frac{2}{3}} A_1^{**}, \quad (9a)$$

$$\mathcal{A}[B^0 \rightarrow K^0 D^{*+} D^{*-}] = \sqrt{\frac{1}{6}} A_1^{**} + \sqrt{\frac{1}{2}} A_0^{**}, \quad (9b)$$

$$\mathcal{A}[B^0 \rightarrow K^+ D^{*0} D^{*-}] = \sqrt{\frac{1}{6}} A_1^{**} - \sqrt{\frac{1}{2}} A_0^{**}, \quad (9c)$$

$$\mathcal{A}[B^+ \rightarrow K^+ D^{*0} \bar{D}^{*0}] = \sqrt{\frac{1}{6}} A_1^{**} + \sqrt{\frac{1}{2}} A_0^{**}, \quad (9d)$$

$$\mathcal{A}[B^+ \rightarrow K^+ D^{*+} D^{*-}] = -\sqrt{\frac{2}{3}} A_1^{**}, \quad (9e)$$

$$\mathcal{A}[B^+ \rightarrow K^0 D^{*+} \bar{D}^{*0}] = \sqrt{\frac{1}{6}} A_1^{**} - \sqrt{\frac{1}{2}} A_0^{**}. \quad (9f)$$

The four amplitudes for the decays into final states that include D^{*0} or \bar{D}^{*0} will be applied to the decays $B \rightarrow KX\pi$ in Section VII.

If the squares of the amplitudes in Eq. (7) are summed over the spin states of any spin-1 charm meson D^* or \bar{D}^* and averaged over the Dalitz plot, the corresponding branching fractions reduce to

$$\text{Br}[B \rightarrow K D^{(*)} \bar{D}^{(*)}] = \frac{\tau[B]}{2M_B} \left| \mathcal{A}[B \rightarrow K D^{(*)} \bar{D}^{(*)}] \right|^2 \Phi_{K D^{(*)} \bar{D}^{(*)}}, \quad (10)$$

where $\tau[B]$ is the lifetime of the B meson and $\Phi_{K D^{(*)} \bar{D}^{(*)}}$ is the integrated 3-body phase space. The ratio of the B^+ and B^0 lifetimes is $\tau[B^+]/\tau[B^0] = 1.076 \pm 0.004$ [14].

A precise isospin analysis of the decays $B \rightarrow K D^{(*)} \bar{D}^{(*)}$ has been presented by Poireau and Zito [25]. The analysis used measurements of 22 branching fractions by the BaBar collaboration [32] and measurements of 2 branching fractions by the Belle collaboration [33, 34]. For each of the four sets of decay channels $K D\bar{D}$, $K D^* \bar{D}$, $K \bar{D}\bar{D}^*$, and $K D^* \bar{D}^*$, Poireau and Zito determined the absolute values and the relative phase of two complex isospin amplitudes A_0 and A_1 by fitting the expressions for the branching fractions in Eqs. (10) to the measurements by the BaBar and Belle collaborations. The isospin amplitudes that appear in Eqs. (8) and (9) are given in Table I.

The separation of scales in the matrix elements for decays $B \rightarrow K D^{(*)} \bar{D}^{(*)}$ would allow them to be expressed as products of short-distance factors involving momenta of order m_π or larger and long-distance factors involving only smaller momentum scales. Summing the squares of matrix elements over the spin states of any D^* or \bar{D}^* and then averaging them over the Dalitz plot, as in the analysis of Ref. [25], decreases their sensitivity to long-distance effects, such as resonances. We will use the constant amplitudes of Poireau and Zito as approximations to short-distance amplitudes for the decays $B \rightarrow K D^{(*)} \bar{D}^{(*)}$ in the region of the Dalitz plot where the charm-meson pair has small relative momentum.

IV. DECAYS INTO K PLUS X

The flavor structure of the $X(3872)$ in Eq. (1) implies that the amplitude for producing X is proportional to the sum of the complex amplitudes for producing $D^{*0}\bar{D}^0$ and $D^0\bar{D}^{*0}$. In the decay of a B meson into $KD^{*0}\bar{D}^0$ or $KD^0\bar{D}^{*0}$ with the charm-meson pair having small relative momentum, the momentum in the charm-meson-pair rest frame of either the incoming B or the outgoing K is about 1550 MeV. Since this momentum is much larger than the pion mass $m_\pi \approx 140$ MeV, the B -to- K transition that creates the charm mesons occurs over distances much shorter than the range $1/m_\pi$ of the interactions between the charm mesons. The interactions between $D^{*0}\bar{D}^0$ and between $D^0\bar{D}^{*0}$ also involve the scale γ_X of the binding momentum of the X , which is much smaller than m_π . The amplitude for the decay can therefore be factored into a long-distance factor that involves γ_X and a short-distance factor that involves only momentum scales of order m_π or larger. In Ref. [35], the inclusive prompt cross sections in high energy hadron collisions for producing $D^{*0}\bar{D}^0$ with small relative momentum and for producing X were expressed in factored forms, with long-distance factors that involve γ_X and short-distance factors that involve only momentum scales of order m_π or larger. The analogous factored form for the exclusive decay rate of B into KX is

$$\Gamma[B \rightarrow KX] = \frac{1}{2M_B} \int d\Phi_{(D^*\bar{D})K} \left| \frac{\mathcal{A}[KD^{*0}\bar{D}^0] + \mathcal{A}[KD^0\bar{D}^{*0}]}{\sqrt{2}} \right|^2 \frac{\Lambda^2 \gamma_X}{4\pi\mu}, \quad (11)$$

where μ is the reduced mass of D^{*0} and \bar{D}^0 and $d\Phi_{(D^*\bar{D})K}$ is the differential two-body phase space for K and a composite particle denoted by $(D^*\bar{D})$ with mass $M_{D^*} + M_{\bar{D}}$. Factors of 3 from the sums over the spin states of D^{*0} or \bar{D}^{*0} are absorbed into the amplitudes \mathcal{A} . The short-distance factor in Eq. (11) involves the short-distance amplitudes $\mathcal{A}[KD^{*0}\bar{D}^0]$ and $\mathcal{A}[KD^0\bar{D}^{*0}]$ for producing $D^{*0}\bar{D}^0$ and $D^0\bar{D}^{*0}$. The short-distance factor also includes the square of an unknown momentum scale Λ of order m_π . The factor Λ^2 is not universal. The corresponding factor in another short-distance production rate may have a different value of order m_π^2 . In the case of inclusive prompt production of X at high-energy hadron colliders, the sums over the many additional particles in the final state wash out the interference between the amplitudes for producing $D^{*0}\bar{D}^0$ and $D^0\bar{D}^{*0}$ and make their contributions to the cross section approximately equal. In the case of exclusive decays of the B meson, the interference effects can be important.

The short-distance amplitudes $\mathcal{A}[KD^{*0}\bar{D}^0]$ and $\mathcal{A}[KD^0\bar{D}^{*0}]$ in Eq. (11) can be expressed in terms of isospin amplitudes as in Eqs. (8). The resulting expressions for the decay rates for $B^+ \rightarrow K^+X$ and $B^0 \rightarrow K^0X$ are

$$\Gamma[B^+ \rightarrow K^+X] = \frac{\lambda^{1/2}(M_B, M_{*0} + M_0, m_K) \Lambda^2 \gamma_X}{768\pi^2 M_B^3 \mu} |A_1^{L*} + A_1^{*L} + \sqrt{3}(A_0^{L*} + A_0^{*L})|^2, \quad (12a)$$

$$\Gamma[B^0 \rightarrow K^0X] = \frac{\lambda^{1/2}(M_B, M_{*0} + M_0, m_K) \Lambda^2 \gamma_X}{192\pi^2 M_B^3 \mu} |A_1^{L*} + A_1^{*L}|^2, \quad (12b)$$

where $\lambda(x, y, z) = (x^4 + y^4 + z^4) - 2(x^2y^2 + y^2z^2 + z^2x^2)$. The ratio of the branching fractions for these decays reduces to

$$\frac{\text{Br}[B^+ \rightarrow K^+X]}{\text{Br}[B^0 \rightarrow K^0X]} = \frac{\tau[B^+]}{\tau[B^0]} \frac{|A_1^{L*} + A_1^{*L} + \sqrt{3}(A_0^{L*} + A_0^{*L})|^2}{4|A_1^{L*} + A_1^{*L}|^2}. \quad (13)$$

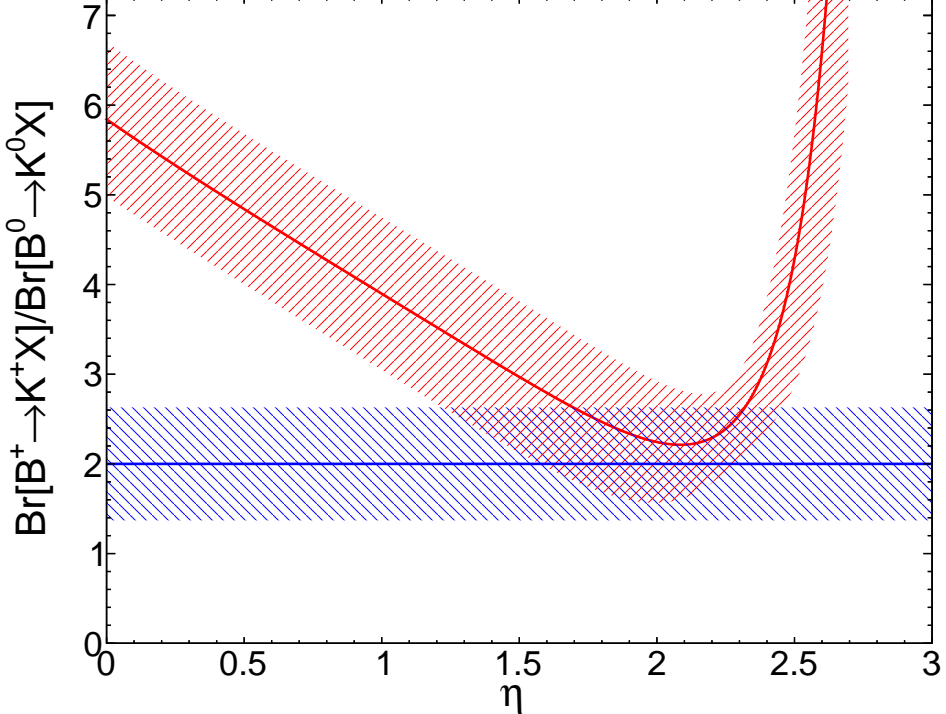


FIG. 1. Ratio of the branching fractions for $B^+ \rightarrow K^+X$ and $B^0 \rightarrow K^0X$ as a function of the angle η in the complex phase of A_1^{L*}/A_1^{*L} . The solid red curve is the theoretical prediction using the central values of the amplitudes in Table I, and the hatched region is the associated error band. The horizontal band is the experimental result in Eq. (14).

An experimental result for the branching ratio in Eq. (13) can be obtained from measurements of the products of the branching fractions for $B \rightarrow KX$ and the branching fraction for $X \rightarrow J/\psi \pi^+ \pi^-$ [14]:

$$\frac{\text{Br}[B^+ \rightarrow K^+X]}{\text{Br}[B^0 \rightarrow K^0X]} = 2.00 \pm 0.63. \quad (14)$$

The theoretical result for the ratio of branching fractions in Eq. (13) depends on the short-distance isospin amplitudes A_0^{L*} , A_1^{L*} , A_0^{*L} , and A_1^{*L} . We will approximate these short-distance isospin amplitudes by the isospin amplitudes determined by the analysis in Ref. [25]. The absolute values of these isospin amplitudes and the complex phases of A_1^{L*}/A_0^{L*} and A_1^{L*}/A_0^{*L} are given with error bars in Table I. The ratio also depends on the complex phase $e^{i\eta}$ of A_1^{L*}/A_1^{*L} , which was not determined in Ref. [25]. We assume for simplicity that all the error bars in Table I and in the ratio $\tau[B^+]/\tau[B^0]$ are uncorrelated Gaussian errors. The ratio of branching fractions in Eq. (13) can then be predicted as a function of η with errors by combining all the errors in quadrature. The theoretical prediction is close to the experimental result in Eq. (14) only if the angle η in the phase factor $e^{i\eta}$ is close to 2. In Fig. 1, the theoretical prediction is shown as a function of η in the region near $\eta = 2$ along with the experimental error band. The difference between the central values in Fig. 1 is the fewest number of standard deviations at $\eta = 2.07$, where the difference is 0.24σ . By requiring the difference between the theoretical prediction and the experimental result to be

less than 1σ , we obtain error bars on the angle η :

$$\eta = 2.07^{+0.30}_{-0.62}. \quad (15)$$

Having determined the angle η in Eq. (15), we can quantify the effects of interference in the decay rates for B mesons into KX in Eq. (11). For B^0 decays, the central values of the squares of the absolute values of the amplitudes $\mathcal{A}[K^0 D^{*0} \bar{D}^0]$, $\mathcal{A}[K^0 D^0 \bar{D}^{*0}]$, and their sum are 0.118, 0.112, and 0.120 times 10^{-10} , respectively. Since the sum of the first two is approximately twice the third, there is substantial destructive interference. For B^+ decays, the central values of the squares of the absolute values of the amplitudes $\mathcal{A}[K^+ D^{*0} \bar{D}^0]$, $\mathcal{A}[K^+ D^0 \bar{D}^{*0}]$, and their sum are 1.11, 0.40, and 0.25 times 10^{-10} , respectively. Since the sum of the first two is much greater than the third, there is large destructive interference.

We proceed to make a quantitative estimate of the branching fraction for $B^0 \rightarrow K^0 X$. After inserting the central values of the isospin amplitudes and η into the decay rate in Eq. (12b), the branching fraction is

$$\text{Br}[B^0 \rightarrow K^0 X] \approx (6.5 \times 10^{-7}) \left(\frac{\Lambda}{m_\pi} \right)^2 \left(\frac{|E_X|}{0.17 \text{ MeV}} \right)^{1/2}. \quad (16)$$

The error in the prefactor from combining the errors in the isospin amplitudes and η in quadrature is more than 100%, with most of the error coming from η . The measured product of this branching fraction with that for the decay of X into $J/\psi \pi^+ \pi^-$ is [14]

$$\text{Br}[B^0 \rightarrow K^0 X] \text{Br}[X \rightarrow J/\psi \pi^+ \pi^-] = (4.3 \pm 1.3) \times 10^{-6}. \quad (17)$$

In Ref. [36], we derived upper and lower bounds on the branching fraction Br for the X bound state to decay into $J/\psi \pi^+ \pi^-$. The loose lower bound $\text{Br} > 4\%$ can be derived from a recent measurement by the BaBar collaboration of the inclusive branching fraction for B^+ into K^+ plus the X resonance feature [37]. An upper bound $\text{Br} < 33\%$ can be derived from measurements of branching ratios of $J/\psi \pi^+ \pi^-$ over other short-distance decay modes of the X . Given the undetermined binding energy $|E_X|$, the large error in the prefactor in Eq. (16), and the uncertainty in the branching fraction for $X \rightarrow J/\psi \pi^+ \pi^-$, the best we can say is that the estimate of the branching fraction for $B^0 \rightarrow K^0 X$ in Eq. (16) is compatible with the measurement in Eq. (17) for some value of Λ of order m_π .

V. HEAVY QUARK SYMMETRIES

The isospin analysis of Poireau and Zito in Ref. [25] exploited the isospin symmetry of QCD. There are other approximate symmetries of QCD that can be used to constrain the matrix elements for the decays $B \rightarrow K D^{(*)} \bar{D}^{(*)}$. One of them is the approximate $SU(3)_L \times SU(3)_R$ chiral symmetry. The K is a pseudo-Goldstone boson associated with the spontaneous breaking of this symmetry, so a matrix element must vanish in the limit as the 4-momentum of K goes to 0. This constraint is automatically satisfied if the matrix element has a factor of the 4-momentum k^μ of K .

Heavy-quark symmetries are approximate symmetries of QCD that relate matrix elements between the 4 sets of channels $K D \bar{D}$, $K D^* \bar{D}$, $K D \bar{D}^*$, and $K D^* \bar{D}^*$. The constraints of heavy-quark symmetries can be expressed most conveniently by arranging the Lorentz-scalar field $D(x)$ for a D and the Lorentz-vector field $D^\mu(x)$ for a D^* into a charm-meson multiplet

field $H^{(c)}(x)$ that is a 4×4 matrix. In momentum space, the spin-1 charm-meson field $D^\mu(p)$ with 4-momentum p satisfies the constraint $p_\mu D^\mu = 0$. The charm-meson multiplet field that creates D or D^* with 4-velocity v and the anticharm-meson multiplet field that creates \bar{D} or \bar{D}^* with 4-velocity \bar{v} are [38]

$$\bar{H}_c^{(c)}(v) = [D_c^\mu(v)^\dagger \gamma_\mu + D_c(v)^\dagger \gamma_5] \frac{1 + \not{v}}{2}, \quad (18a)$$

$$\bar{H}_d^{(\bar{c})}(\bar{v}) = \frac{1 - \not{\bar{v}}}{2} [\bar{D}_d^\mu(\bar{v})^\dagger \gamma_\mu + \bar{D}_d(\bar{v})^\dagger \gamma_5]. \quad (18b)$$

The subscripts c and d are the isospin indices of the isospin-doublet fields. The multiplet fields satisfy $\bar{H}_c^{(c)} \not{v} = \bar{H}_c^{(c)}$ and $\not{v} \bar{H}_d^{(\bar{c})} = -\bar{H}_d^{(\bar{c})}$. An interaction term that produces the decay $B \rightarrow K D^{(*)} \bar{D}^{(*)}$ must have a factor of the B -meson field B_a . It is convenient to express the field that annihilates the B meson with 4-velocity v_B as a 4×4 matrix obtained by setting the B^* field to zero in the antibottom-meson multiplet field:

$$H_a^{(\bar{b})}(v_B) = [-B_a(v_B) \gamma_5] \frac{1 - \not{v}_B}{2}. \quad (19)$$

This field satisfies $H_a^{(\bar{b})} \not{v}_B = -H_a^{(\bar{b})}$. An interaction term that produces the decay $B \rightarrow K D^{(*)} \bar{D}^{(*)}$ must also have a factor of the kaon field K_b^\dagger . The Goldstone nature of the K requires the matrix element to have a factor of its 4-momentum k^μ . The Lorentz index of k^μ can be contracted with that of a Dirac matrix γ^μ . Lorentz-invariant interaction terms can be expressed as Dirac traces of products of $H_a^{(\bar{b})}(v_B)$, $\bar{H}_c^{(c)}(v)$, $\bar{H}_d^{(\bar{c})}(\bar{v})$ and Dirac matrices in which all Lorentz indices are contracted.

Voloshin has pointed out that the even charge conjugation of the $X(3872)$ together with the S-wave nature of the dominant $D^{*0} \bar{D}^0$ and $D^0 \bar{D}^{*0}$ components of its wavefunction imply that the $c\bar{c}$ pair must be in a spin-triplet state [39]. Since the B decays into KX , the amplitudes for B to decay into $K D^* \bar{D}$ and $K D \bar{D}^*$ must have a substantial component in which the $c\bar{c}$ pair is in a spin-triplet state near the point on the edge of the Dalitz plot where the charm mesons have equal 4-velocities. The simplest way to deduce the behavior of an interaction term under rotations of the heavy-quark spins is through a nonrelativistic reduction using the methods of Ref. [40]. Interaction terms for which the $c\bar{c}$ pair is in a spin-triplet state can be constructed by requiring the charm-meson multiplet fields to appear in the combination $\bar{H}_c^{(c)} \gamma^\mu \bar{H}_d^{(\bar{c})}$. The simplest such interaction terms that are nonzero when the charm mesons have equal 4-velocities are

$$\frac{1}{M_B} \text{Tr} \left[\bar{H}_c^{(c)}(v) \gamma^\mu \bar{H}_d^{(\bar{c})}(v) \left(B_{abcd} H_a^{(\bar{b})}(v_B) + C_{abcd} [H_a^{(\bar{b})}(v_B), \gamma_5] \right) \right] k_\mu K_b(k)^\dagger, \quad (20)$$

where the complex coefficients B_{abcd} and C_{abcd} are dimensionless. Interaction terms for which the $c\bar{c}$ pair is in a spin-singlet state when the charm mesons have equal 4-velocities can be constructed by requiring the charm-meson multiplet fields to appear in the combination $\bar{H}_c^{(c)} \gamma^5 \bar{H}_d^{(\bar{c})}$.

Conservation of electric charge implies that there are 6 sets of subscripts for which the coefficients B_{abcd} and C_{abcd} are nonzero. Isospin symmetry can be used to reduce each set of coefficients B_{abcd} and C_{abcd} in Eq. (20) to two complex isospin coefficients that correspond to $D^{(*)}K$ with total isospin quantum number 0 or 1. The nonzero coefficients B_{abcd} are linear combinations of isospin coefficients B_0 and B_1 analogous to the linear combinations of

isospin amplitudes on the right sides of Eqs. (8) and (9), and similarly for C_{abcd} . With isospin symmetry, the interaction terms in Eq. (20) are determined by the 4 isospin coefficients B_0 , B_1 , C_0 , and C_1 .

It is possible that the interaction terms in Eq. (20) for which the $c\bar{c}$ pair is in a spin-triplet state when the charm mesons have equal 4-velocities actually dominate. We will refer to this possibility as *spin-triplet dominance*. In the isospin analysis in Ref. [25], Poireau and Zito determined 2 constant complex amplitudes that determine 6 decay rates for each of the 4 sets of channels $KD\bar{D}$, $KD^*\bar{D}$, $KD\bar{D}^*$, and $KD^*\bar{D}^*$. Since one can choose phases so that one of each pair of amplitudes is real, there are 12 real parameters. The assumption of spin-triplet dominance gives interaction terms with 4 complex isospin coefficients that determine the amplitudes for all the channels $KD\bar{D}$, $KD^*\bar{D}$, $KD\bar{D}^*$, and $KD^*\bar{D}^*$. Since one coefficient can be chosen to be real, there are 7 real coefficients. They might provide enough freedom to reproduce the 12 real parameters in the isospin analysis of Ref. [25] to within the errors. The results of that isospin analysis could certainly be reproduced by adding interaction terms for which the $c\bar{c}$ pair is in a spin-singlet state when the charm mesons have equal 4-velocities.

The matrix elements that correspond to the spin-triplet interaction terms in Eq. (20) can be determined by evaluating the Dirac traces. The matrix elements are Lorentz-invariant functions of the 4-momenta P , p , \bar{p} , k (with $P = p + \bar{p} + k$) and the polarization 4-vectors ε and $\bar{\varepsilon}$ of D^* and \bar{D}^* (which satisfy $p \cdot \varepsilon = 0$ and $\bar{p} \cdot \bar{\varepsilon} = 0$). At the point on the edge of the Dalitz plot where the charm mesons have equal 4-velocities, the matrix elements reduce to

$$\mathcal{A}[B \rightarrow K D \bar{D}] = -C \frac{\lambda(M_B, 2M_D, m_K)}{8M_B^2 M_D^2}, \quad (21a)$$

$$\mathcal{A}[B \rightarrow K D^* \bar{D}] = -B \frac{(M_B + M_{D^*} + M_D)^2 - m_K^2}{2M_B^2 (M_{D^*} + M_D)} P \cdot \varepsilon, \quad (21b)$$

$$\mathcal{A}[B \rightarrow K D \bar{D}^*] = -B \frac{(M_B + M_{D^*} + M_D)^2 - m_K^2}{2M_B^2 (M_{D^*} + M_D)} P \cdot \bar{\varepsilon}, \quad (21c)$$

$$\begin{aligned} \mathcal{A}[B \rightarrow K D^* \bar{D}^*] = & -C \left(\frac{\lambda(M_B, 2M_{D^*}, m_K)}{8M_B^2 M_{D^*}^2} \varepsilon \cdot \bar{\varepsilon} + \frac{4}{M_B^2} P \cdot \varepsilon P \cdot \bar{\varepsilon} \right) \\ & + iB \frac{(M_B + 2M_{D^*})^2 - m_K^2}{8M_B^2 M_{D^*}^2} \epsilon_{\mu\nu\alpha\beta} P^\mu k^\nu \varepsilon^\alpha \bar{\varepsilon}^\beta. \end{aligned} \quad (21d)$$

On the left side, we have suppressed the isospin indices a , b , c , and d of the mesons B , K , $D^{(*)}$, and $\bar{D}^{(*)}$. On the right side, we have suppressed the subscripts $abcd$ of the coefficients B and C . The nonzero coefficients can be expressed in terms of isospin coefficients B_0 , B_1 , C_0 , and C_1 .

VI. DECAYS INTO K PLUS $D^* \bar{D}^*$ NEAR THRESHOLD

In the decay of a B meson into $K D^* \bar{D}^*$ with the pair of spin-1 charm mesons having small relative momentum, the momentum in the charm-meson-pair rest frame of either the incoming B or the outgoing K is about 1350 MeV. Since this is much larger than m_π , the B -to- K transition occurs over distances much shorter than the range $1/m_\pi$ of the interactions between the charm mesons. As far as the D^* and \bar{D}^* are concerned, the $B \rightarrow K$ transition can be described as a point interaction that creates D^* and \bar{D}^* . The amplitude for producing

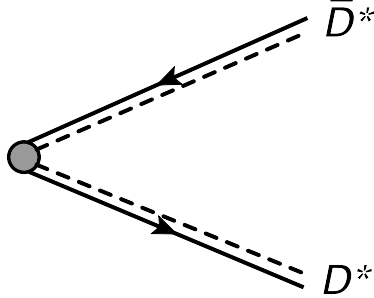


FIG. 2. Feynman diagram in XEFT for production of $D^* \bar{D}^*$ from their creation at a point. The D^* and \bar{D}^* are represented by double lines consisting of a dashed line and a solid line with an arrow.

$D^* \bar{D}^*$ can be represented in XEFT by the Feynman diagram in Fig. 2 with a vertex from which the D^* and \bar{D}^* emerge. The vertex factor for the B -to- K transition that creates $D^* \bar{D}^*$ at a point is $i\mathcal{A}^{ij}[KD^* \bar{D}^*]$, where i and j are the spin indices of the D^* and \bar{D}^* . The vertex factor \mathcal{A}^{ij} is a Cartesian tensor in the center-of-momentum (CM) frame of $D^* \bar{D}^*$. The only preferred direction is that of the 3-momentum \mathbf{P} of the decaying B meson, which is also the direction of the 3-momentum of the final-state K . The amplitude must therefore have the tensor structure

$$\mathcal{A}^{ij}[B \rightarrow KD^* \bar{D}^*] = D \delta^{ij} + E \hat{P}^i \hat{P}^j + iF \epsilon^{ijk} \hat{P}^k, \quad (22)$$

where the complex coefficients D , E , and F are dimensionless. We have suppressed the isospin indices a , b , c , and d of the mesons B , K , $D^{(*)}$, and $\bar{D}^{(*)}$ and the subscripts $abcd$ of the coefficients D , E , and F . The nonzero coefficients D_{abcd} can be expressed as linear combinations of two isospin coefficients D_0 and D_1 analogous to the linear combinations in Eqs. (9), and similarly for E_{abcd} and F_{abcd} . If we make the approximation of spin-triplet dominance that gives the Lorentz-invariant amplitude in Eq. (21d), the coefficients are

$$D_i \approx C_i \frac{\lambda(M_B, 2M_{D^*}, m_K)}{8M_B^2 M_{D^*}^2}, \quad (23a)$$

$$E_i \approx -C_i \frac{\lambda(M_B, 2M_{D^*}, m_K)}{4M_B^2 M_{D^*}^2}, \quad (23b)$$

$$F_i \approx B_i \frac{[(M_B + 2M_{D^*})^2 - m_K^2] \lambda^{1/2}(M_B, 2M_{D^*}, m_K)}{16M_B^2 M_{D^*}^2}. \quad (23c)$$

Note that the assumption of spin-triplet dominance implies $E_i = -2D_i$.

The matrix element for producing $D^* \bar{D}^*$ is obtained by contracting the tensor $\mathcal{A}^{ij}[KD^* \bar{D}^*]$ with the polarization vectors ε^i and $\bar{\varepsilon}^j$ of the D^* and \bar{D}^* . If the amplitude \mathcal{A}^{ij} in Eq. (22) is contracted with $\varepsilon^i \bar{\varepsilon}^j$, multiplied by its complex conjugate, and then summed over the spin states of D^* and \bar{D}^* , the result is

$$|\mathcal{A}[KD^* \bar{D}^*]|^2 \equiv \sum_{\text{spins}} |\varepsilon^i \mathcal{A}^{ij} \bar{\varepsilon}^j|^2 = 2|D|^2 + |D + E|^2 + 2|F|^2. \quad (24)$$

We use the symbol $|\mathcal{A}[KD^* \bar{D}^*]|^2$ as a concise notation for the sum in Eq. (24), and we refer to it as a *squared amplitude*, even though it is actually a sum of squares. For any specific decay channel $KD^* \bar{D}^*$, D can be expressed as the same linear combination of isospin coefficients

D_0 and D_1 as in Eqs. (9), and similarly for E and F . For the decays that produce D^{*0} , the resulting expressions for the squared amplitudes are

$$|\mathcal{A}[K^0 D^{*0} \bar{D}^{*0}]|^2 = \frac{2(2|D_1|^2 + |D_1 + E_1|^2 + 2|F_1|^2)}{3}, \quad (25a)$$

$$|\mathcal{A}[K^+ D^{*0} D^{*-}]|^2 = \frac{2|D_1 - \sqrt{3}D_0|^2 + |D_1 + E_1 - \sqrt{3}(D_0 + E_0)|^2 + 2|F_1 - \sqrt{3}F_0|^2}{6}, \quad (25b)$$

$$|\mathcal{A}[K^+ D^{*0} \bar{D}^{*0}]|^2 = \frac{2|D_1 + \sqrt{3}D_0|^2 + |D_1 + E_1 + \sqrt{3}(D_0 + E_0)|^2 + 2|F_1 + \sqrt{3}F_0|^2}{6}. \quad (25c)$$

These squared amplitudes depend on 10 independent real components of the 6 isospin coefficients. The squared amplitude $|\mathcal{A}[K^0 D^{*+} \bar{D}^{*0}]|^2$ is equal to $|\mathcal{A}[K^+ D^{*0} D^{*-}]|^2$ by isospin symmetry.

The differential decay rates for producing $D^* \bar{D}^*$ with small relative momentum can be obtained by multiplying the squared amplitudes, such as those in Eqs. (25), by the differential phase space for $K D^* \bar{D}^*$ and by $1/2M_B$. If the amplitudes do not vary dramatically across the Dalitz plot, the resulting expressions for the differential decay rates may also be reasonable approximations throughout the Dalitz plot. In this case, the squared amplitudes in Eqs. (25) can be approximated by the squares of the corresponding amplitudes in Eqs. (9). The isospin amplitudes A_0^{**} and A_1^{**} from the isospin analysis of Poireau and Zito in Ref. [25] are given by the last row of Table I. Inserting them into the amplitudes in Eqs. (9a), (9c), and (9d), and then evaluating their absolute squares, we obtain

$$|\mathcal{A}[K^0 D^{*0} \bar{D}^{*0}]|^2 = (0.35 \pm 0.05) \times 10^{-10}, \quad (26a)$$

$$|\mathcal{A}[K^+ D^{*0} D^{*-}]|^2 = (2.85 \pm 0.22) \times 10^{-10}, \quad (26b)$$

$$|\mathcal{A}[K^+ D^{*0} \bar{D}^{*0}]|^2 = (2.52 \pm 0.21) \times 10^{-10}. \quad (26c)$$

These equations provide 3 real constraints on the 6 complex isospin coefficients in Eqs. (25).

The squared amplitudes in Eqs. (25) can be simplified by assuming the spin-triplet dominance of the amplitudes, which implies $E_i = -2D_i$. They then reduce to

$$|\mathcal{A}[K^0 D^{*0} \bar{D}^{*0}]|^2 \approx 2|D_1|^2 + \frac{4}{3}|F_1|^2, \quad (27a)$$

$$|\mathcal{A}[K^+ D^{*0} D^{*-}]|^2 \approx \frac{1}{2}|D_1 - \sqrt{3}D_0|^2 + \frac{1}{3}|F_1 - \sqrt{3}F_0|^2, \quad (27b)$$

$$|\mathcal{A}[K^+ D^{*0} \bar{D}^{*0}]|^2 \approx \frac{1}{2}|D_1 + \sqrt{3}D_0|^2 + \frac{1}{3}|F_1 + \sqrt{3}F_0|^2. \quad (27c)$$

These squared amplitudes depend on 6 independent real components of the 6 complex isospin coefficients. The values of the squared amplitudes in Eqs. (26) provide 3 real constraints.

VII. DECAYS INTO K PLUS X AND A PION

A pair of spin-1 charm mesons $D^* \bar{D}^*$ created at short distances with relative momentum \mathbf{k} can rescatter into $X(3872)\pi$ with relative momentum \mathbf{q} . The rescattering can be described within XEFT provided the relative momentum of the charm mesons that form the X is less than about m_π . The Feynman diagrams for $D^* \bar{D}^*$ created at a point to rescatter into $X\pi$

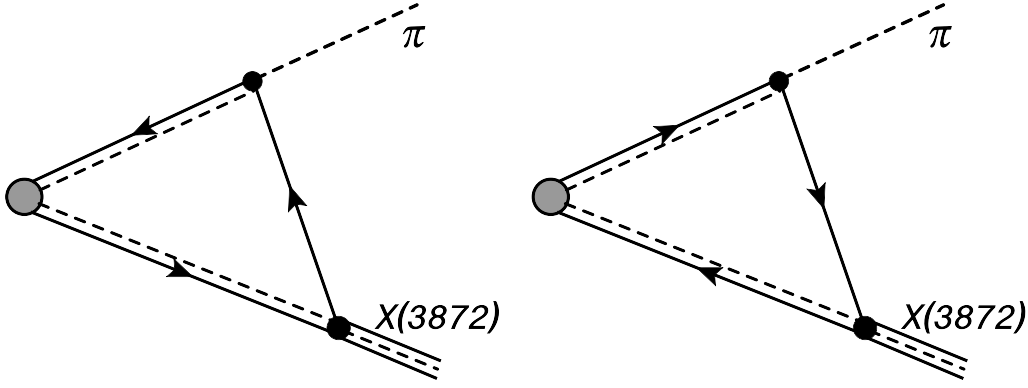


FIG. 3. Feynman diagrams in XEFT for $D^* \bar{D}^*$ created at a point to rescatter into $X\pi$. The D and \bar{D} are represented by solid lines with an arrow. The X is represented by a triple line consisting of two solid lines and one dashed line. The π is represented by a dashed line.

are shown in Fig. 3. These diagrams can be calculated using the Feynman rules for Galilean-invariant XEFT in Ref. [29] together with the vertices for the coupling of $D^{*0} \bar{D}^0$ and $D^0 \bar{D}^{*0}$ to X in Ref. [16]. These vertices are given by $(\sqrt{\pi\gamma_X}/\mu)\delta^{ij}$, where i and j are the spin indices of the spin-1 charm meson and the X .

In the case of the production of $X\pi^0$ from $D^{*0} \bar{D}^{*0}$ created at short distances, the amplitude is given by the sum of the two diagrams in Fig. 3. The integral over the loop energy is conveniently evaluated by contours using the pole of the propagator for the D^* or \bar{D}^* line attached to the X . The remaining two propagators can be combined into a single denominator by introducing an integral over a Feynman parameter x . The integral over the loop momentum can be evaluated analytically. Our result for the amplitude for producing $X\pi^0$ with small relative momentum \mathbf{q} and with polarization vector $\boldsymbol{\varepsilon}$ for the X is

$$i\mathcal{A}^{ij}[KD^{*0} \bar{D}^{*0}]\frac{g(\pi\gamma_X M_{*0}^3/m_0)^{1/2}}{16\pi\mu f_\pi}(\varepsilon^i q^j + q^i \varepsilon^j) \int_0^1 dx \left(\frac{2M_0}{2M_0 + (1-x)m_0}\right)^{5/2} \times \left[(\delta_0 - \gamma_X^2/2\mu) - (1+x)(\delta_0 - i\Gamma_{*0}/2) + \frac{M_0 x}{(2M_0 + (1-x)m_0)\mu_{X\pi}} \mathbf{q}^2 \right]^{-1/2}, \quad (28)$$

where $\delta_0 = M_{*0} - M_0 - m_0 = 7.0$ MeV, $\Gamma_{*0} \approx 60$ keV is the predicted decay width of D^{*0} [29], and $\mu_{X\pi} = ((2M_0 + m_0)m_0)/(2(M_0 + m_0))$ is the Galilean-invariant reduced mass of $X\pi$. The coupling constant for the pion-emission vertex is $g/(2\sqrt{m_0}f_\pi) = 0.30/m_0^{3/2}$ [29]. The final integral over x can also be evaluated analytically if the integrand is simplified using $m_0 \ll M_0$. Our final result for the amplitude is relatively simple:

$$i\mathcal{A}^{ij}[KD^{*0} \bar{D}^{*0}]\frac{g(\pi\gamma_X M_{*0}^3/m_0)^{1/2}}{8\pi\mu f_\pi} \frac{\varepsilon^i q^j + q^i \varepsilon^j}{\sqrt{q^2/2m_0 - \delta_0 - \gamma_X^2/2\mu + i\Gamma_{*0}} + \sqrt{-\gamma_X^2/2\mu + i\Gamma_{*0}/2}}. \quad (29)$$

The denominator is a kinematic singularity factor that would have a zero at $q^2 = 2m_0\delta_0$ if the binding momentum γ_X and the width Γ_{*0} were both zero. The kinematic singularity is called a *triangle singularity*, because it arises from the region where the three charm meson lines that form a triangle in the Feynman diagrams in Fig. 3 are all simultaneously on shell.

In the case of the production of $X\pi^-$ from $D^{*0} \bar{D}^{*-}$ created at short distances, the amplitude is given by the first diagram in Fig. 3 only. The coupling constant for the pion-emission

vertex is $g/(\sqrt{2m_0}f_\pi)$. If the loop integral is simplified using $m_0 \ll M_0$, our final result for the amplitude for producing $X\pi^-$ with small relative momentum \mathbf{q} and with polarization vector $\boldsymbol{\varepsilon}$ for the X is

$$i\mathcal{A}^{ij}[KD^{*0}D^{*-}]\frac{g(2\pi\gamma_X M_{*0}^3/m_0)^{1/2}}{8\pi\mu f_\pi} \times \frac{\varepsilon^i q^j}{\sqrt{q^2/2m_0 - \delta_1 - \gamma_X^2/2\mu + i(\Gamma_{*0} + \Gamma_{*1})/2} + \sqrt{-\gamma_X^2/2\mu + i\Gamma_{*0}/2}}, \quad (30)$$

where $\delta_1 = M_{*1} - M_0 - m_1 = 5.9$ MeV and $\Gamma_{*1} \approx 83$ keV is the measured decay width of D^{*-} . The amplitude for producing $X\pi^+$ from $D^{*+}\bar{D}^{*0}$ created at short distances can be obtained by replacing the vertex factor by $\mathcal{A}^{ij}[KD^{*+}\bar{D}^{*0}]$ and replacing $\varepsilon^i q^j$ by $q^i \varepsilon^j$. The denominator of Eq. (30) is a triangle-singularity factor that would have a zero at $q^2 = 2m_0\delta_1$ if the binding momentum γ_X and the widths Γ_{*0} and Γ_{*1} were all zero.

Our expressions for the amplitudes in Eqs. (29) and (30) should be accurate provided the momentum integral that results in Eq. (28) is dominated by regions where the relative momentum \mathbf{k} of the charm mesons that form the X is less than about m_π . This condition imposes a constraint on the relative momentum \mathbf{q} of X and π . The constraint can be deduced from the integrated expression in Eq. (28) by requiring the energy proportional to \mathbf{q}^2 inside the last factor to be less than $m_\pi^2/2\mu$. At $x = 1$, this energy is $E_{X\pi} = q^2/2\mu_{X\pi}$. Thus the kinetic energy $E_{X\pi}$ must be less than about $m_\pi^2/2\mu \approx 10$ MeV.

To obtain the differential decay rate for producing $X\pi$ with small relative momentum, the amplitude in Eq. (29) or (30) must be multiplied by its complex conjugate, summed over the spin states of X , and then multiplied by the differential phase space for $KX\pi$ and by $1/2M_B$. The differential decay rate for producing $X\pi$ with relative momentum \mathbf{q} is

$$d\Gamma[B \rightarrow KX\pi] = \frac{1}{2M_B} \int d\Phi_{(D^*\bar{D}^*)K} \left| \mathcal{A}[KX\pi] \right|^2 \frac{d^3q}{(2\pi)^3 2\mu_{X\pi}}, \quad (31)$$

where $d\Phi_{(D^*\bar{D}^*)K}$ is the differential two-body phase space for K and a composite particle denoted by $(D^*\bar{D}^*)$ with mass $2M_{D^*}$. The differential decay rate can be simplified by averaging over the directions of \mathbf{q} or, equivalently, by averaging over the directions of the momentum \mathbf{P} of B . The average of the product of the amplitude \mathcal{A}^{ij} in Eq. (22) and its complex conjugate $(\mathcal{A}^{kl})^*$ over the directions of the momentum of the B is

$$\langle \mathcal{A}^{ij}(\mathcal{A}^{kl})^* \rangle = \left| D + \frac{1}{3}E \right|^2 \delta^{ij} \delta^{kl} + \frac{1}{15}|E|^2 (\delta^{ik} \delta^{jl} + \delta^{il} \delta^{jk} - \frac{2}{3} \delta^{ij} \delta^{kl}) + \frac{1}{3}|F|^2 (\delta^{ik} \delta^{jl} - \delta^{il} \delta^{jk}). \quad (32)$$

If the amplitude \mathcal{A}^{ij} in Eq. (22) is contracted with the tensors in the numerators of Eqs. (29) and (30), multiplied by its complex conjugate, and then summed over the spin states of X , the results are

$$\sum_{\text{spins}} \langle \mathcal{A}^{ij}(\mathcal{A}^{kl})^* \rangle (\varepsilon^i q^j + q^i \varepsilon^j)(\varepsilon^k q^l + q^k \varepsilon^l)^* = 4 \left(\left| D + \frac{1}{3}E \right|^2 + \frac{2}{9}|E|^2 \right) \mathbf{q}^2, \quad (33a)$$

$$\sum_{\text{spins}} \langle \mathcal{A}^{ij}(\mathcal{A}^{kl})^* \rangle (\varepsilon^i q^j)(\varepsilon^k q^l)^* = \left(\left| D + \frac{1}{3}E \right|^2 + \frac{2}{9}|E|^2 + \frac{2}{3}|F|^2 \right) \mathbf{q}^2. \quad (33b)$$

For any specific decay channel $KX\pi$, the coefficient D can be expressed as the same linear combination of isospin coefficients D_0 and D_1 as in Eqs. (9), and similarly for E and F . We

introduce a compact notation for the factors that depend on the isospin coefficients:

$$|\mathcal{A}[K^0 X \pi^0]|^2 \equiv |D_1 + \frac{1}{3}E_1|^2 + \frac{2}{9}|E_1|^2, \quad (34a)$$

$$|\mathcal{A}[K^+ X \pi^-]|^2 \equiv |D_1 + \frac{1}{3}E_1 - \sqrt{3}(D_0 + \frac{1}{3}E_0)|^2 + \frac{2}{9}|E_1 - \sqrt{3}E_0|^2 + \frac{2}{3}|F_1 - \sqrt{3}F_0|^2, \quad (34b)$$

$$|\mathcal{A}[K^+ X \pi^0]|^2 \equiv |D_1 + \frac{1}{3}E_1 + \sqrt{3}(D_0 + \frac{1}{3}E_0)|^2 + \frac{2}{9}|E_1 + \sqrt{3}E_0|^2, \quad (34c)$$

$$|\mathcal{A}[K^0 X \pi^+]|^2 \equiv |D_1 + \frac{1}{3}E_1 - \sqrt{3}(D_0 + \frac{1}{3}E_0)|^2 + \frac{2}{9}|E_1 - \sqrt{3}E_0|^2 + \frac{2}{3}|F_1 - \sqrt{3}F_0|^2. \quad (34d)$$

Note that $|\mathcal{A}[K^0 X \pi^+]|^2$ is equal to $|\mathcal{A}[K^+ X \pi^-]|^2$. We refer to these factors as squared amplitudes, even though they are actually sums of squares.

The differential decay rates for B^0 into $K^0 X \pi^0$ and into $K^+ X \pi^-$ with small relative momentum \mathbf{q} for $X\pi$ are

$$\begin{aligned} \frac{d\Gamma}{d^3q}[B^0 \rightarrow K^0 X \pi^0] &= |\mathcal{A}[K^0 X \pi^0]|^2 \frac{g^2 \lambda^{1/2}(M_B, 2M_{D^*}, m_K) M_{D^*}^3 \gamma_X}{96(2\pi)^5 M_B^3 \mu^2 f_\pi^2 \mu_{X\pi}} \\ &\times \frac{q^2/2m_0}{|\sqrt{q^2/2m_0 - \delta_0 - \gamma_X^2/2\mu + i\Gamma_{*0}} + \sqrt{-\gamma_X^2/2\mu + i\Gamma_{*0}/2}|^2}, \end{aligned} \quad (35a)$$

$$\begin{aligned} \frac{d\Gamma}{d^3q}[B^0 \rightarrow K^+ X \pi^-] &= |\mathcal{A}[K^+ X \pi^-]|^2 \frac{g^2 \lambda^{1/2}(M_B, 2M_{D^*}, m_K) M_{D^*}^3 \gamma_X}{768(2\pi)^5 M_B^3 \mu^2 f_\pi^2 \mu_{X\pi}} \\ &\times \frac{q^2/2m_0}{|\sqrt{q^2/2m_0 - \delta_1 - \gamma_X^2/2\mu + i(\Gamma_{*0} + \Gamma_{*1})/2} + \sqrt{-\gamma_X^2/2\mu + i\Gamma_{*0}/2}|^2}. \end{aligned} \quad (35b)$$

The differential decay rate for $B^+ \rightarrow K^+ X \pi^0$ differs from that for $B^0 \rightarrow K^0 X \pi^0$ only by an overall multiplicative factor that depends on isospin coefficients, while the differential decay rate for $B^+ \rightarrow K^0 X \pi^+$ is the same as that for $B^0 \rightarrow K^+ X \pi^-$:

$$\frac{d\Gamma}{d^3q}[B^+ \rightarrow K^+ X \pi^0] = \frac{|\mathcal{A}[K^+ X \pi^0]|^2}{4|\mathcal{A}[K^0 X \pi^0]|^2} \frac{d\Gamma}{d^3q}[B^0 \rightarrow K^0 X \pi^0], \quad (36a)$$

$$\frac{d\Gamma}{d^3q}[B^+ \rightarrow K^0 X \pi^+] = \frac{d\Gamma}{d^3q}[B^0 \rightarrow K^+ X \pi^-]. \quad (36b)$$

The differential decay rates in Eqs. (35) can be expressed as differential branching fractions $d\text{Br}/dE_{X\pi}$ in the kinetic energy $E_{X\pi} = q^2/2\mu_{X\pi}$ of X and π in their CM frame. Their normalizations depend on the undetermined coefficients D_i , E_i , and F_i , but their dependence on $E_{X\pi}$ is predicted. The shapes of the differential branching fractions for the decays of B^0 into $K^0 X \pi^0$ and $K^+ X \pi^-$ are illustrated in Fig. 4 for X with binding energy 0.17 MeV. The normalizations of the curves are arbitrary. Both of the curves have a narrow peak from a charm-meson triangle singularity. The $B \rightarrow K$ transition creates a pair of charm mesons $D^* \bar{D}^*$ that are almost on shell, one of them decays into $D\pi$ or $\bar{D}\pi$, and the resulting pair of almost on-shell charm mesons binds to form the X . For the decay $B^0 \rightarrow K^0 X \pi^0$, there is a narrow peak in $E_{X\pi}$ near $\delta_0 = 7.0$ MeV. The peak is produced by the denominator in Eq. (35a). The full width at half maximum of that factor is $1.17 \gamma_X^2/2\mu$ if the binding energy $\gamma_X^2/2\mu$ is large compared to Γ_{*0} and $6.21 \Gamma_{*0} \approx 370$ keV if $\gamma_X^2/2\mu$ is small compared to Γ_{*0} . For the decay $B^0 \rightarrow K^+ X \pi^-$, there is a narrow peak in $E_{X\pi}$ near $\delta_1 = 5.9$ MeV. The peak is produced by the denominator in Eq. (35b). The full width at half maximum of that factor in Eq. (35b) is $1.17 \gamma_X^2/2\mu$ if $\gamma_X^2/2\mu$ is large compared to Γ_{*0} and Γ_{*1} and approximately 430 keV if $\gamma_X^2/2\mu$ is small compared to Γ_{*0} and Γ_{*1} .

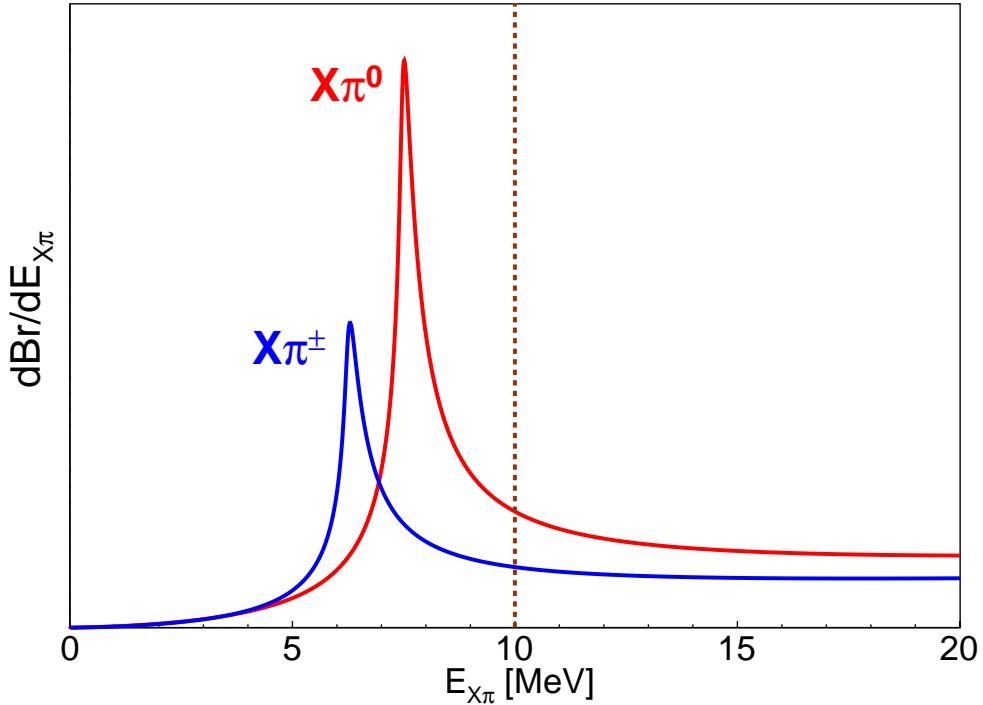


FIG. 4. Differential branching fractions $dBr/dE_{X\pi}$ for the decays $B^0 \rightarrow K^0 X\pi^0$ and $B^+ \rightarrow K^+ X\pi^0$ (taller red curve) and $B^0 \rightarrow K^+ X\pi^-$ and $B^+ \rightarrow K^0 X\pi^+$ (shorter blue curve) as functions of the kinetic energy $E_{X\pi} = q^2/2\mu_{X\pi}$ of $X\pi$ in its CM frame. The binding energy of the X is 0.17 MeV. The region of validity of XEFT extends out to about the vertical dotted line at $E_{X\pi} = 10$ MeV. The normalizations of the curves are arbitrary. The relative normalizations of the $X\pi^0$ and $X\pi^\pm$ curves are chosen so their extrapolations to large $E_{X\pi}$ are equal.

At energies above the narrow peaks, our expressions for the differential branching fractions $dBr/dE_{X\pi}$ in Eqs. (35a) and (35b) have local minima at energies $E_{X\pi}$ near $3\delta_0$ and $3\delta_1$, respectively. At higher energies, the distributions increase as $E_{X\pi}^{1/2}$. This differs from the behavior $E_{X\pi}^{3/2}$ expected from the P-wave coupling of the pion because of the resonance factors in the denominators of the amplitudes in Eqs. (35). The region of $E_{X\pi}$ where the distributions increase is beyond the energy $m_\pi^2/2\mu$ where XEFT breaks down, which is marked by a vertical dotted line in Fig. 4.

The contributions of the triangle singularities to the integrated decay rates can be estimated by integrating the momentum distributions in Eqs. (35) from the threshold to some energy $E_{\max} = q_{\max}^2/2\mu_{X\pi}$ beyond the peak. In the limits $\Gamma_{*0} \rightarrow 0$ and $\gamma_X \ll \sqrt{\mu\delta_0}$, the integral of the momentum dependent factor in Eq. (35a) over the region $|\mathbf{q}| < q_{\max}$ is

$$\int_{q < q_{\max}} \frac{d^3q}{(2\pi)^3} \frac{q^2/2m_0}{\left| \sqrt{q^2/2m_0 - \delta_0 - \gamma_X^2/2\mu + i\epsilon} + i\sqrt{\gamma_X^2/2\mu} \right|^2} = \frac{1}{2\pi^2} (2m_0\delta_0)^{3/2} \times \left[\log \frac{8\mu\delta_0}{\gamma_X^2} + \frac{1}{3} \left(\frac{q_{\max}^2}{2m_0\delta_0} \right)^{3/2} + \left(\frac{q_{\max}^2}{2m_0\delta_0} \right)^{1/2} - \frac{1}{2} \log \frac{\sqrt{q_{\max}^2/2m_0\delta_0} + 1}{\sqrt{q_{\max}^2/2m_0\delta_0} - 1} - \frac{11}{3} \right]. \quad (37)$$

The coefficient of $(2m_0\delta_0)^{3/2}$ diverges logarithmically as $\gamma_X \rightarrow 0$. If we do not take the limit $\Gamma_{*0} \rightarrow 0$, the coefficient of $(m_0\delta_0)^{3/2}$ also depends logarithmically on Γ_{*0} . In the limit

$\Gamma_{*0} \rightarrow 0$ and $\Gamma_{*1} \rightarrow 0$, the integral of the momentum dependent factor in Eq. (35b) is given by Eq. (37) with δ_0 replaced by δ_1 .

The normalizations factors in the differential decay rates in Eqs. (35) and (36) depend on the unknown isospin coefficients D_i , E_i , and F_i . The normalization factors can be simplified by assuming the spin-triplet dominance of the amplitudes, which implies $E_i = -2D_i$. The three distinct squared amplitudes in Eqs. (34) then reduce to

$$|\mathcal{A}[K^0 X \pi^0]|^2 \approx |D_1|^2, \quad (38a)$$

$$|\mathcal{A}[K^+ X \pi^-]|^2 \approx |D_1 - \sqrt{3}D_0|^2 + \frac{2}{3}|F_1 - \sqrt{3}F_0|^2, \quad (38b)$$

$$|\mathcal{A}[K^+ X \pi^0]|^2 \approx |D_1 + \sqrt{3}D_0|^2. \quad (38c)$$

These expressions are related in a simple way to the corresponding expressions for the squared amplitudes for $B \rightarrow KD^*\bar{D}^*$ in Eqs. (27). Using the numerical estimates in Eqs. (26), we obtain the estimate

$$|\mathcal{A}[K^+ X \pi^-]|^2 = |\mathcal{A}[K^0 X \pi^+]|^2 \approx 5.7 \times 10^{-10}. \quad (39)$$

We also obtain the upper bounds

$$|\mathcal{A}[K^0 X \pi^0]|^2 < 0.17 \times 10^{-10}, \quad (40a)$$

$$|\mathcal{A}[K^+ X \pi^0]|^2 < 5.0 \times 10^{-10}. \quad (40b)$$

We can use the squared amplitudes in Eq. (39) to estimate branching fractions for decays of B into $KX\pi$, with $X\pi$ in the peak from the triangle singularity. We denote the region of the peak by $(X\pi)_\Delta$. We declare that region to be $E_{X\pi}$ from 0 up to $E_{\max} = 2\delta_0 = 14.0$ MeV for $(X\pi^0)_\Delta$ and up to $E_{\max} = 2\delta_1 = 11.8.0$ MeV for $(X\pi^\pm)_\Delta$. We approximate the integrals over the momentum distributions in Eqs. (35a) and (35b) using the integral in Eq. (37) and the analogous integral with δ_0 replaced by δ_1 . The resulting estimate of the branching fraction for $B^0 \rightarrow K^+(X\pi^-)_\Delta$ as a function of the binding energy $|E_X| = \gamma_X^2/2\mu$ is

$$\text{Br}[B^0 \rightarrow K^+(X\pi^-)_\Delta] \approx (2.4 \times 10^{-7}) \left(\frac{|E_X|}{0.17 \text{ MeV}} \right)^{1/2} \left[2.64 - \log \frac{|E_X|}{0.17 \text{ MeV}} \right]. \quad (41)$$

Our estimate of the branching fraction for $B^+ \rightarrow K^0(X\pi^+)_\Delta$ is larger by the ratio $\Gamma[B^0]/\Gamma[B^+]$ = 1.08 of the decay widths. We get an upper bound on the branching fraction for $B^0 \rightarrow K^0(X\pi^0)_\Delta$:

$$\text{Br}[B^0 \rightarrow K^0(X\pi^0)_\Delta] < (8 \times 10^{-8}) \left(\frac{|E_X|}{0.17 \text{ MeV}} \right)^{1/2} \left[2.82 - \log \frac{|E_X|}{0.17 \text{ MeV}} \right]. \quad (42)$$

Our upper bound on the branching fraction for $B^+ \rightarrow K^+(X\pi^0)_\Delta$ differs only by the replacement of the prefactor by 6×10^{-7} .

The Belle collaboration has observed the decay of B^0 into $K^+ X \pi^-$ [41]. The product of the branching fraction for the B^0 decay and the branching fraction for the decay $X \rightarrow J/\psi \pi^+ \pi^-$ was measured to be $(7.9 \pm 1.3 \pm 0.4) \times 10^{-6}$. Some of the decays come from $B^0 \rightarrow K^{*0} X$ followed by the decay of the $K^*(892)$ resonance into $K^+ \pi^-$. The fraction of events that proceed through the K^{*0} resonance is $(34 \pm 9 \pm 2)\%$ [41]. Our estimate of the branching fraction for $B^0 \rightarrow K^+(X\pi^-)_\Delta$ in Eq. (41) implies that the narrow peak from the charm-meson triangle singularity can contribute an observable fraction of the decays into $K^+ X \pi^-$ provided the binding energy of the X is not too much smaller than 0.17 MeV.

VIII. DISCUSSION

We have studied the production of $X(3872)$ accompanied by a pion in exclusive decays $B \rightarrow KX\pi$. This reaction can proceed through the decay of B at short distances into K plus a $D^*\bar{D}^*$ pair with small relative momentum followed by the rescattering of $D^*\bar{D}^*$ into $X\pi$. We used a precise isospin analysis of the decays $B^0 \rightarrow KD^{(*)}\bar{D}^{(*)}$ by Poireau and Zito [25] to obtain approximations for the short-distance amplitudes for these decays. We verified that those amplitudes are consistent with the measured ratio of the branching fractions for $B^+ \rightarrow K^+X$ and $B^0 \rightarrow K^0X$, as can be seen in Fig. 1. We used XEFT to calculate the amplitude for the rescattering of $D^*\bar{D}^*$ into $X\pi$. The distributions of the kinetic energy $E_{X\pi}$ of X and π in the $X\pi$ CM frame are given in Eqs. (35) and (36), and their shapes are illustrated in Fig. 4. The distribution in $E_{X\pi}$ has a narrow peak near the $D^*\bar{D}^*$ threshold from a charm-meson triangle singularity. For the decays $B^0 \rightarrow K^0X\pi^0$ and $B^+ \rightarrow K^+X\pi^0$, the peak in $E_{X\pi}$ is predicted to be near $\delta_0 = 7.0$ MeV. For the decays $B^0 \rightarrow K^+X\pi^-$ and $B^+ \rightarrow K^0X\pi^+$, the peak is predicted to be near $\delta_1 = 5.9$ MeV.

The normalization factors in our $X\pi$ kinetic energy distributions in Eqs. (35) and (36) depend on short-distance coefficients in the amplitudes for $B \rightarrow KD^*\bar{D}^*$ in Eq. (22). They can be related to coefficients of Lorentz-invariant interaction terms constrained by heavy quark-spin symmetry, such as those in Eq. (20). The simplifying assumption of spin-triplet dominance, which gives the interaction terms in Eq. (20), could be eliminated by adding interaction terms for which the $c\bar{c}$ pair is in a spin-singlet state when the charm mesons have equal 4-velocities. The coefficients of the interaction terms could be determined by squaring the amplitudes $\mathcal{A}[B \rightarrow KD^{(*)}\bar{D}^{(*)}]$, summing over spins, averaging over the Dalitz plot, and fitting to the results of Ref. [25]. This would give more reliable estimates of the branching fractions for the decays of B into KX plus a soft pion. An important limitation of the isospin analysis of Poireau and Zito is that it assumed that the amplitudes were constant across the Dalitz plot. A more ambitious approach would be to take into account the variations of the amplitudes across the Dalitz plot by fitting the coefficients of the interaction terms to results from Dalitz plot analyses of all the decays $B \rightarrow KD^{(*)}\bar{D}^{(*)}$. The BaBar collaboration has carried out Dalitz plot analyses of the decays $B^0 \rightarrow K^+D^0D^-$ and $B^+ \rightarrow K^+D^0\bar{D}^0$ [42].

The region of validity of our expressions for the differential branching fractions in Eqs. (35) and (36) is limited to kinetic energy $E_{X\pi}$ less than about $m_\pi^2/2\mu \approx 10$ MeV. The calculations could be extended to larger $E_{X\pi}$ using a strategy applied to $e^+e^- \rightarrow X\gamma$ in Ref. [43]. After integrating over the loop energy, the amplitudes from the Feynman diagrams in Fig. 3 can be expressed in a form in which the product of the vertex for the coupling of the X to the charm mesons and the propagators for those two charm mesons is replaced by the momentum-space wavefunction for the X with momentum \mathbf{q} . The results we have presented correspond to the simple wavefunction $\psi(k)$ for X in its rest frame in Eq. (3), whose region of validity is limited to $k \ll m_\pi$. The wavefunction at k of order m_π could presumably be calculated using XEFT. Such a wavefunction could be used to extend the calculation of the rate for $B \rightarrow KX\pi$ to larger $E_{X\pi}$. For $E_{X\pi}$ larger than about $m_\pi^2/2\mu_{X\pi} \approx 75$ MeV, it is also necessary to use relativistic kinematics for the pion.

We used the assumption of spin-triplet dominance to estimate the branching fractions for decays of B into K plus $X\pi$ in the peak from the charm-meson triangle singularity, which we denoted by $(X\pi)_\Delta$. Our estimate for $B^0 \rightarrow K^+(X\pi^-)_\Delta$, which applies also to $B^+ \rightarrow K^0(X\pi^+)_\Delta$, is given in Eq. (41). We only obtained upper bounds on the branching fractions for $B^0 \rightarrow K^0(X\pi^0)_\Delta$ and $B^+ \rightarrow K^0(X\pi^+)_\Delta$. These estimates and upper bounds

are essentially proportional to the square root of the binding energy E_X of the X . The Belle experiment at KEK accumulated roughly $7.7 \times 10^8 B\bar{B}$ events. The BaBar experiment at SLAC accumulated roughly $4.7 \times 10^8 B\bar{B}$ events. Our estimates of the branching fractions for $B \rightarrow K(X\pi)_\Delta$ suggest that it may be possible to observe the narrow peak from the charm-meson triangle singularity in the previous data from those experiments provided the binding energy of the X is not too much smaller than 0.17 MeV. The prospects are even better at the Belle II experiment at SuperKEKB, which may be able to achieve a luminosity 40 times larger than the Belle experiment. The observation of a peak in the $X\pi$ invariant mass distribution near the $D^*\bar{D}^*$ threshold would provide strong support for the identification of X as a weakly bound charm-meson molecule and present a serious challenge to other models.

ACKNOWLEDGMENTS

This work was supported in part by the Department of Energy under grant DE-SC0011726 and by the National Science Foundation under grant PHY-1607190. We thank R. Kass for useful information.

- [1] H.X. Chen, W. Chen, X. Liu and S.L. Zhu, The hidden-charm pentaquark and tetraquark states, *Phys. Rept.* **639**, 1 (2016) [arXiv:1601.02092].
- [2] A. Hosaka, T. Iijima, K. Miyabayashi, Y. Sakai and S. Yasui, Exotic hadrons with heavy flavors: X , Y , Z , and related states, *PTEP* **2016**, 062C01 (2016) [arXiv:1603.09229].
- [3] R.F. Lebed, R.E. Mitchell and E.S. Swanson, Heavy-Quark QCD Exotica, *Prog. Part. Nucl. Phys.* **93**, 143 (2017) [arXiv:1610.04528].
- [4] A. Esposito, A. Pilloni and A.D. Polosa, Multiquark Resonances, *Phys. Rept.* **668** (2017) 1 [arXiv:1611.07920].
- [5] F.K. Guo, C. Hanhart, U.G. Meißner, Q. Wang, Q. Zhao and B. S. Zou, Hadronic molecules, *Rev. Mod. Phys.* **90**, 015004 (2018) [arXiv:1705.00141].
- [6] A. Ali, J.S. Lange and S. Stone, Exotics: Heavy Pentaquarks and Tetraquarks, *Prog. Part. Nucl. Phys.* **97**, 123 (2017) [arXiv:1706.00610].
- [7] S.L. Olsen, T. Skwarnicki and D. Zieminska, Nonstandard heavy mesons and baryons: Experimental evidence, *Rev. Mod. Phys.* **90**, 015003 (2018) [arXiv:1708.04012].
- [8] M. Karliner, J.L. Rosner and T. Skwarnicki, Multiquark States, *Ann. Rev. Nucl. Part. Sci.* **68**, 17 (2018) [arXiv:1711.10626].
- [9] C.Z. Yuan, The XYZ states revisited, *Int. J. Mod. Phys. A* **33**, 1830018 (2018) [arXiv:1808.01570].
- [10] N. Brambilla, S. Eidelman, C. Hanhart, A. Nefediev, C.P. Shen, C.E. Thomas, A. Vairo and C.Z. Yuan, The XYZ states: experimental and theoretical status and perspectives, arXiv:1907.07583 [hep-ex].
- [11] S.K. Choi *et al.* [Belle Collaboration], Observation of a narrow charmonium-like state in exclusive $B^\pm \rightarrow K^\pm \pi^+ \pi^- J/\psi$ decays, *Phys. Rev. Lett.* **91**, 262001 (2003) [hep-ex/0309032].
- [12] K. Abe *et al.* [Belle Collaboration], Evidence for $X(3872) \rightarrow \gamma J/\psi$ and the sub-threshold decay $X(3872) \rightarrow \omega J/\psi$, hep-ex/0505037.
- [13] R. Aaij *et al.* [LHCb Collaboration], Determination of the $X(3872)$ meson quantum numbers, *Phys. Rev. Lett.* **110**, 222001 (2013) [arXiv:1302.6269].

- [14] M. Tanabashi *et al.* [Particle Data Group], Review of Particle Physics, Phys. Rev. D **98**, 030001 (2018).
- [15] S. Fleming, M. Kusunoki, T. Mehen and U. van Kolck, Pion interactions in the $X(3872)$, Phys. Rev. D **76**, 034006 (2007) [hep-ph/0703168].
- [16] E. Braaten, H.-W. Hammer and T. Mehen, Scattering of an Ultrasoft Pion and the $X(3872)$, Phys. Rev. D **82**, 034018 (2010) [arXiv:1005.1688].
- [17] E. Braaten, L.-P. He and K. Ingles, Production of $X(3872)$ Accompanied by a Pion at Hadron Colliders, arXiv:1903.04355 [hep-ph].
- [18] A.P. Szczepaniak, Triangle Singularities and XYZ Quarkonium Peaks, Phys. Lett. B **747**, 410 (2015) [arXiv:1501.01691].
- [19] X.H. Liu, M. Oka and Q. Zhao, Searching for observable effects induced by anomalous triangle singularities, Phys. Lett. B **753**, 297 (2016) [arXiv:1507.01674].
- [20] A.P. Szczepaniak, Dalitz plot distributions in presence of triangle singularities, Phys. Lett. B **757**, 61 (2016) [arXiv:1510.01789].
- [21] F. K. Guo, Traps in hadron spectroscopy: Thresholds, triangle singularities, ..., PoS Hadron **2017**, 015 (2018) [arXiv:1712.10126].
- [22] F.K. Guo, Novel method for precisely measuring the $X(3872)$ mass, Phys. Rev. Lett. **122**, 202002 (2019) [arXiv:1902.11221].
- [23] S. Dubynskiy and M.B. Voloshin, $e^+e^- \rightarrow \gamma X(3872)$ near the $D^*\bar{D}^*$ threshold, Phys. Rev. D **74**, 094017 (2006) [hep-ph/0609302].
- [24] E. Braaten, L.-P. He and K. Ingles, Triangle Singularity in the Production of $X(3872)$ and a Photon in e^+e^- Annihilation, Phys. Rev. D **100**, 031501 (2019) [arXiv:1904.12915].
- [25] V. Poireau and M. Zito, A precise isospin analysis of $B \rightarrow \bar{D}^{(*)}D^{(*)}K$ decays, Phys. Lett. B **704**, 559 (2011) [arXiv:1107.1438].
- [26] E. Braaten and H.-W. Hammer, Universality in few-body systems with large scattering length, Phys. Rept. **428**, 259 (2006) [cond-mat/0410417].
- [27] E. Braaten and M. Kusunoki, Factorization in the production and decay of the $X(3872)$, Phys. Rev. D **72**, 014012 (2005) [hep-ph/0506087].
- [28] V. Baru, A.A. Filin, C. Hanhart, Y.S. Kalashnikova, A.E. Kudryavtsev and A.V. Nefediev, Three-body $D\bar{D}\pi$ dynamics for the $X(3872)$, Phys. Rev. D **84**, 074029 (2011) [arXiv:1108.5644].
- [29] E. Braaten, Galilean-invariant effective field theory for the $X(3872)$, Phys. Rev. D **91**, 114007 (2015) [arXiv:1503.04791].
- [30] M. Schmidt, M. Jansen and H.-W. Hammer, Threshold Effects and the Line Shape of the $X(3872)$ in Effective Field Theory, Phys. Rev. D **98**, 014032 (2018) [arXiv:1804.00375].
- [31] M. Zito, Isospin analysis of $B \rightarrow \bar{D}^{(*)}D^{(*)}K$ decays, Phys. Lett. B **586**, 314 (2004) [hep-ph/0401014].
- [32] P. del Amo Sanchez *et al.* [BaBar Collaboration], Measurement of the $B \rightarrow \bar{D}^{(*)}D^{(*)}K$ branching fractions, Phys. Rev. D **83**, 032004 (2011) [arXiv:1011.3929].
- [33] J. Dalseno *et al.* [Belle Collaboration], Measurement of Branching Fraction and Time-Dependent CP Asymmetry Parameters in $B^0 \rightarrow D^{*+}D^{*-}K_s^0$ Decays, Phys. Rev. D **76**, 072004 (2007) [arXiv:0706.2045].
- [34] J. Brodzicka *et al.* [Belle Collaboration], Observation of a new D_{sJ} meson in $B^+ \rightarrow \bar{D}^0D^0K^+$ decays, Phys. Rev. Lett. **100**, 092001 (2008) [arXiv:0707.3491].
- [35] P. Artoisenet and E. Braaten, Production of the $X(3872)$ at the Tevatron and the LHC, Phys. Rev. D **81**, 114018 (2010) [arXiv:0911.2016].

- [36] E. Braaten, L.-P. He and K. Ingles, Branching Fractions of the $X(3872)$, arXiv:1908.02807 [hep-ph].
- [37] G. Wormser (on behalf of the BaBar collaboration), presented at Quarkonium 2019 in Torino, May 2019.
- [38] B. Grinstein, E.E. Jenkins, A.V. Manohar, M.J. Savage and M.B. Wise, Chiral perturbation theory for f_{D_s}/f_D and B_{B_s}/B_B , Nucl. Phys. B **380**, 369 (1992) [hep-ph/9204207].
- [39] M.B. Voloshin, Heavy quark spin selection rule and the properties of the $X(3872)$, Phys. Lett. B **604**, 69 (2004) [hep-ph/0408321].
- [40] J. Hu and T. Mehen, Chiral Lagrangian with heavy quark-diquark symmetry, Phys. Rev. D **73**, 054003 (2006) [hep-ph/0511321].
- [41] A. Bala *et al.* [Belle Collaboration], Observation of $X(3872)$ in $B \rightarrow X(3872) K\pi$ decays, Phys. Rev. D **91**, 051101 (2015) [arXiv:1501.06867].
- [42] J. P. Lees *et al.* [BaBar Collaboration], Dalitz plot analyses of $B^0 \rightarrow D^- D^0 K^+$ and $B^+ \rightarrow \bar{D}^0 D^0 K^+$ decays, Phys. Rev. D **91**, 052002 (2015) [arXiv:1412.6751].
- [43] E. Braaten, L.-P. He and K. Ingles, Production of $X(3872)$ and a Photon in e^+e^- Annihilation, [arXiv:1909.03901 [hep-ph]].